Assessment of flow pattern and mixing phenomena in alumina digesters

Kiran Bhor[1], Kumaresan T.[2], Ashish Mishra[3], Narinder Walia[4], Sudip Bhattacharya[5]
1. Scientist
2. Senior Scientist
Aditya Birla Science and Technology Company Pvt. Limited, Navi Mumbai, India
3. Senior Engineer
4. General Manager
5. Joint President and Unit Head
Hindalco Industries Limited, Muri, India
Corresponding author: kumaresan.t@adityabirla.com

Abstract

In Bayer process, alumina is extracted from bauxite by double digestion process followed by precipitation of green liquor and calcination of hydrate particles to produce metallurgical grade alumina. In general, industry scale high temperature digesters are equipped with a multi-stage agitator design. Apart from the agitator, digester internal design plays a vital role that determines the quality of flow and in turn, affects the extraction efficiency of bauxite digestion. Short circuiting (channelling), excess back mixing of slurry, and formation of dead zones are the common engineering challenges faced by taller aspect ratio digester designs. The current analysis is focused on investigation and assessment of the effect of digester internal design on the flow pattern and mixing phenomena using computational fluid dynamics (CFD) modeling and validated using flow visualization experiments.

Keywords: Bayer process digester; digester agitator design; CFD modelling of Bayer process digesters; Dispersion number; *E* curve.

1. Introduction

The Hindalco alumina refineries in India are based on the Bayer process technology. The refinery is basically classified into two major areas called redside and whiteside. The technology has to follow four important steps in the Bayer process for the production of alumina i.e., grinding and digestion, solid-liquid separation, precipitation and calcination. Digestion is the unit process that is vital in determining the productivity from the redside of the technology. The main raw material input for the digestion area of an alumina plant is the bauxite slurry coming from the pre-desilication, or slurry storage processes. The bauxite at the Muri refinery has boehmite content varying from 8 to 12 %, hence high temperature digesters are needed to recover boehmite content succeeding the gibbsite digestion. The primary chemical reaction in high temperature digestion is as follows

$$Al_2O_3.H_2O + 2\mathrm{NaOH} \xrightarrow{245^oC} 2\mathrm{Na}AlO_2 + 2H_2O \qquad \textbf{(1)}$$

During the high temperature dissolution process, the alumina from bauxite gets dissolved in the Bayer liquor in the form of sodium aluminate and the insoluble residue (red mud) will be separated from sodium aluminate in the subsequent clarification operation. In general, the effectiveness of the dissolution process strongly depends upon the reaction kinetics, hydrodynamics and physical operating conditions prevailing in the digestor. The reaction chemistry of the alumina extraction is a function of minerals association in the bauxite, grain phase size distribution and type of overall mineral chemistry composition. However, for the given bauxite quality, operating conditions and hydrodynamics in the digester can always be

altered to favor the maximum extraction efficiency with an economic recovery. One of the major focus for today's alumina refineries must be to improve the energy efficiency due to the current variation of specific energy consumption of global alumina refineries from 7 to 24 GJ/T. Further, the energy consumption is particularly design specific with respect to digestion and calcination which together account for more than seventy percentage of refinery thermal energy consumption. So it is imperative to look into the detailed design of the digester to obtain a maximum extraction efficiency. The effectiveness of the digester varies dramatically from one design to the other. The design variations could be with respect to the shape and size of the digester, inlet/outlet (location, orientation, and shape), internals design (baffles, impeller type, impeller shape and impeller size) and with respect to agitator speed [1, 2]. This implies that hydrodynamics plays a major role in an industry scale effective dissolution process for the given bauxite quality. In the past decade, CFD has become a vibrant tool to optimize the process designs in the hydrometallurgical industries; especially the alumina industries [3 – 5]. In the present work, an attempt has been made to assess and validate the flow and mixing pattern of bauxite slurry in the high temperature digesters.

2. CFD modeling and simulation

Even though CFD simulation is becoming increasingly popular among hydrometallurgical industries [3, 4, 6]; few literature references are available specific to alumina digester analysis. [4] successfully modelled the digester slurry hydrodynamics as a single phase to study the influence of vessel aspect ratio and inlet configuration for the selection of preferred vessel geometry. Also, [2] simulated the hydrodynamics of bauxite slurry in the low temperature digesters assuming a homogeneous and non-settling slurry. In the present analysis, similar physical properties have been considered for the bauxite slurry. Figure 1 shows three digesters.

The geometry and the tetrahedral meshing is done using ANSYS-ICEM 14 and numerical simulations are carried out using ANSYS-Fluent 14. The turbulence is modeled using a single phase realizable k-ε model. This model provides a superior performance for flows involving rotation, boundary layers under strong adverse pressure gradients, separation and recirculation against the standard k-ε turbulence model. The 3D computational tetrahedral elements are around 600 000 for the present digester design. The modeled transport equations for k and ε in the realizable k-ε model are as follows

$$\frac{\partial}{\partial t}(\rho k) + \frac{\partial}{\partial x_i}(\rho k u_j) = \frac{\partial}{\partial x_i}\left[\left(\mu + \frac{\mu_t}{\sigma_k}\right)\frac{\partial k}{\partial x_j}\right] + G_k + G_b - \rho\epsilon - Y_M + S_k \quad \textbf{(2)}$$

$$\frac{\partial}{\partial t}(\rho\epsilon) + \frac{\partial}{\partial x_j}(\rho\epsilon u_j) = \frac{\partial}{\partial x_j}\left[\left(\mu + \frac{\mu_t}{\sigma_k}\right)\frac{\partial \epsilon}{\partial x_j}\right] + \rho C_1 S_\epsilon + \rho C_2 \frac{\epsilon^2}{k + \sqrt{\nu\epsilon}} + C_{1_\epsilon}\frac{\epsilon}{k}C_{3_\epsilon}G_b + S_\epsilon \quad \textbf{(3)}$$

where:

$$C_1 = max\left[0.43, \frac{\eta}{\eta+5}\right] \; and \; \eta = \frac{k}{\epsilon} \quad (3a)$$

In the case of the standard k-ε model, the eddy viscosity, μ_t has a constant C_μ value whereas the realizable k-ε model has C_μ, which is dependent upon the mean strain and rotation rates, the angular velocity of the impeller rotation and turbulence fields, k and ε. In the literature, it was found that the realizable k-ε model extensively validated for a wide range of flows i.e., rotating

homogeneous shear flows, free flows including jets and mixing layers, channel and boundary layer flows, and separated flows. Hence, it is decided to carry out the simulations using the realizable k-ε model. Also, it was observed from the literature that the performance of the model is substantially better than that of the standard k-ε model.

The impeller rotation is modeled by moving reference frame technique along with the realizable k-ε turbulence model. For the estimation of RTD, the transport equation for the concentration c (scalar) was simulated. After computation of the velocity information and turbulence characteristics, the tracer blending process was modeled by solving the tracer conservation equation. Here, the dispersive transport of the tracer due to turbulent motion in the reactor is accounted by the turbulent diffusivity. A simple dispersion model is used to predict the axial dispersion. In any continuous unit operation/processes, as soon as the pulse tracer is introduced into the vessel, the pulse spreads with respect to the nature of the flow pattern and finally it exits from the outlet of the digestor. The two main important parameters to be observed are the mean residence time, t_m and variance of the tracer, σ^2 [7]. The deviation from the plug flow is characterized by the dispersion number, D/uL. The E curve is created using the following equation.

$$E = \frac{1}{\sqrt{4\pi(D/uL)}} exp\left[\frac{t_m\left((1-(t/t_m)\right)^2}{4t(D/uL)}\right] \quad \textbf{(4)}$$

The parameter E is nothing but the normalized exit age distribution function. The purpose of keeping it normalized is that the flow distribution inside the reactors of different scales can be compared directly. [3], validated their CFD based RTD with the lithium ion tracer experiments for refinery thickeners. The successful predictions show the validation of a CFD model.

Table 1. Pumping efficiency of agitator from CFD.

Digester with baffles with 46 rpm				$\langle N_P \rangle = 12.38$	
Impeller design	N_P	N_{QP}	N_{QS}	E_P	E_T
DT1	2.11	0.683	0.972	0.151	0.434
DT2	2.22	0.678	0.946	0.14	0.381
DT3	2.22	0.681	0.953	0.142	0.390
DT4	2.21	0.662	0.949	0.131	0.386
DT5	2.28	0.674	1.106	0.134	0.592
PBTD	1.32	1.07	2.241	0.924	8.488
Digester without baffles with 46 rpm				$\langle N_P \rangle = 10.81$	
DT1	1.8	0.679	1.004	0.174	0.561
DT2	1.89	0.713	1.108	0.191	0.718
DT3	1.89	0.715	1.113	0.193	0.728
DT4	1.88	0.695	1.095	0.178	0.695
DT5	2.16	0.694	1.09	0.154	0.597
PBTD	1.16	1.036	2.142	0.957	8.458

Figure 1 shows the industry scale geometric setup of the digester with and without baffle that is used for CFD analysis. Figure 1A depicts the digester with three vertical baffles placed at 90^o orientation to each other and agitator rotation of 46 rpm. Figure 1B depicts the same design as seen in Figure 1A, but with zero agitator rotation. Figure 1C depicts the digester design without baffles and with agitator rotation of 46 rpm. The 0 rpm case was deliberately considered to

understand the impact of agitator rotation on the overall flow pattern and mixing. The presence of arrow mark around the shaft on the figure 1A and 1C indicates that the agitator is rotating at 46 rpm.

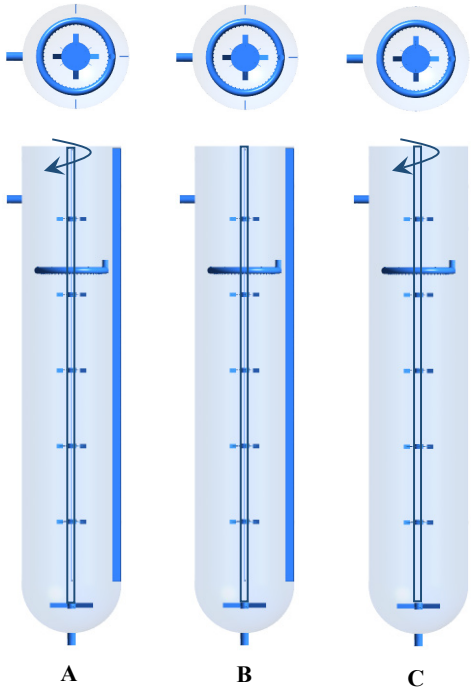

Figure 1. Plan and orthographic view of digester designs (A) Digester with baffles with 46 rpm (B) Digester with baffles with 0 rpm (C) Digester without baffles with 46 rpm.

Table 2. RTD analysis by CFD.

Design	Retention time (s)	Dispersion Number, D/uL
Digester with baffle with 46 RPM	2076	0.189
Digester with baffle with 0 RPM	2002	0.215
Digester w/o baffle with 46 RPM	2268	0.201

3. Flow visualization experiments (Torque, Velocity and RTD)

The industry scale high temperature digester is geometrically scaled down by 1/12th from the original size for performing flow visualization experiments to validate CFD predictions. Appropriately, all internals are scaled down and flow experiments are conducted with the same level of power per unit volume (P/V). The scale down setup is a transparent acrylic vessel in which water is used as a working fluid. The setup is fabricated in such a way that all internals can be modified for further design modification and optimization analysis. The entire assembly is mounted on the torque table that measures the load imparted by the fluid motion. The power number of the agitator is calculated following the measurement of torque.

Power number, $N_P = \frac{2\pi N\tau}{\langle P \rangle}$ **(5)**

Agitator power consumption, $\langle P \rangle = \rho N^3 D^5$ **(6)**

The noninvasive velocity measurements are carried out using ultrasonic velocity profiler (UVP, Met-flow Swiss made) at various locations in the scale down digester setup. The polystyrene particles are used as seeding particles in the working fluid to reflect the echo of ultrasonic pulses transmitted from the probe. Also, seeding particles are selected in such a manner that they

follow the flow path of the working fluid. As soon as the ultrasound wave hits particles, it gets reflected with a frequency shift. Since the UVP probe acts both as a transmitter as well as a receiver, it measures the time and frequency shift of ultrasonic wave, and the signal is used to calculate both the velocity and direction of particles. The mean radial velocities from the periphery of the impeller in the tangential direction are used for the calculation of flow numbers for DT. Similarly, the mean axial velocities below the impeller plane, in the radial direction, are used for the calculation of flow numbers for PBTD. The primary flow number *(N_{QP})* and secondary flow number *(N_{QS})* were calculated using the following equations

Primary flow number for DT, $$N_{QP} = \frac{\int_0^{2\pi} \int_{B_B}^{B_T} rU_r dz d\theta}{ND^3} \quad (7)$$

Secondary flow number for DT, $$N_{QS} = \frac{\int_0^{2\pi} \int_{B_{BE}}^{B_{TE}} rU_r dz d\theta}{ND^3} \quad (8)$$

Primary flow number for PBTD, $$N_{QP} = \frac{\int_0^{2\pi} \int_0^{R_I} rU_z dr d\theta}{ND^3} \quad (9)$$

Secondary flow number for PBTD, $$N_{QS} = \frac{\int_0^{2\pi} \int_0^{R_R} rU_z dr d\theta}{ND^3} \quad (10)$$

The conductivity probe (Honeywell toroidal type) located at the outlet location of the scaled down setup measures the electrical conductivity of spread tracer. Sodium chloride mixed with blue colour dyed solution is used as tracer and injected at the inlet location. The conductivity data is calibrated for the tracer concentration and the exit age distribution is plotted using equation 4.

4. Extent of digestion

The flow and the mixing (RTD) pattern of the digester depends on the operating conditions and equipment design. Accordingly, the mean retention time and extent of dispersion are calculated from the hydrodynamics. The extent of boehmite digestion and the extent of dissolution of aluminium ions from the solid phase will be dependent upon the flow environment. The boehmite dissolution rate is slower than gibbsite dissolution and is chemical reaction controlled [8, 9]. The conversion or extent of reaction is determined by the equation below as calculated by the [4] for kaolinite dissolution.

$$X = 1 - \frac{4a.exp\left(\frac{1}{2D/uL}\right)}{(1+a^2).exp\left(\frac{a}{2D/uL}\right)-(1-a^2).exp\left(\frac{a}{2D/uL}\right)} \quad \textbf{(11)}$$

where: $a = \sqrt{1 + 4\kappa\tau(D/uL)}$ and assuming boehmite reaction rate constant (κ) as 0.00076 s^{-1} in the present study.

5. Results and discussions

In the Bayer alumina process, most of the process equipment are built with taller aspect ratio i.e., the H/T ratio is always greater than 1. The high temperature digester considered in the present work has an aspect ratio of H/T ~ 4. The hydrodynamics of the digester are in general complex with chaotic turbulence along with high temperature solid-liquid reactions. However,

CFD simulations in the present work are carried out to study the flow and mixing phenomena without accounting for the boehmite and caustic reactions. In the high temperature digester, the quality of mixing mainly depends upon the relative distribution of mean and turbulent kinetic energy. One extreme is the absence of turbulence and the entire energy exists in the form of mean kinetic energy. The other extreme is that the flow is turbulent at all the locations and the mean velocities are zero. Obviously, the actual flow in the digester will be in between the two extremes, and will depend upon impeller design, diameter and the location of impeller, tank design, tank diameter and internals such as steam injection tubes, baffles etc.

Figure 2 depicts the overall flow velocity vectors in the digesters. It can be observed that there are totally six impellers (DT1, DT2, DT3, DT4, DT5 and PBTD towards outlet) attached to the shaft of the agitator in all three designs considered for the present study. The DT are the radial flow type impeller that will pump the slurry in the radial outward direction. However, beyond the impeller zone, the principal radial direction may vary and is dependent upon the design of other internals. The PBTD are the axial flow type impellers that will pump the slurry in the downward axial direction.

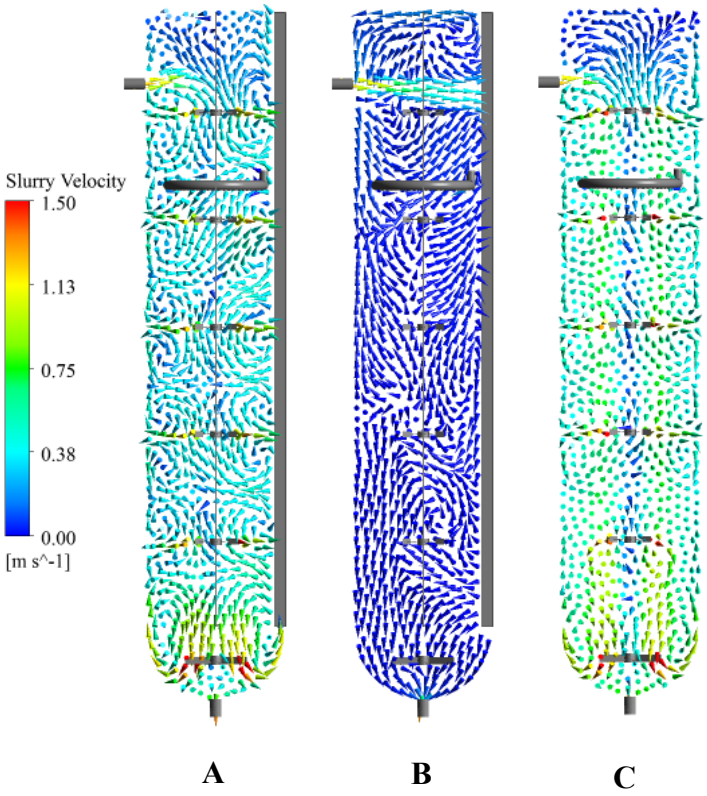

Figure 2. Velocity vectors in digesters (A) Digester with baffles with 46 rpm (B) Digester with baffles with 0 rpm (C) Digester without baffles with 46 rpm.

Figure 2A shows that overall velocity vectors for the digester design with baffles and agitator rotating at 46 rpm. It can be observed that the radial jet from the DT impellers hits the digester wall and take many axial recirculation loops. The velocity magnitude varies from 1.5 m/s near the periphery of the impeller zones to 0.38 m/s in the major free zones away from the impeller. Once these radial jets hits and dissipates energy near the digester wall, the vertical baffles will guide the flow to change the direction of the diverged jet both in the upward and downward axial direction. So the integrated effect of interaction of all diverged jets from all five radial flow impellers will cause several axial recirculation vortices in the majority volume of the digester. Also, it can be clearly observed that the PBTD impeller in the bottom portion of the

digester produces an axial jet and the same hits the digester wall at 45°. This axial jet pushes the flow towards the outlet of the digester and creates relatively a longer axial recirculation loops in the dish shaped bottom zone of the digester.

Table 3. Stage wise conversion by CFD.

κ, **Rate constant** 0.00076 (s^{-1})

Digester with baffles with 46 RPM			
Zone	**τ (s)**	**D/uL**	**X (%)**
DT1	1119	0.598	49.94
DT2	1382	0.918	54.82
DT3	1629	0.315	63.44
DT4	1818	0.254	67.71
DT5	2008	0.204	71.68
PBTD	2075	0.189	72.99
Outlet	2076	0.189	73.00
Digester with baffles with 0 RPM			
DT1	1213	0.483	52.93
DT2	1377	0.399	57.38
DT3	1560	0.336	61.85
DT4	1952	0.253	69.90
DT5	1972	0.246	70.33
PBTD	1869	0.235	68.89
Outlet	2002	0.215	71.37
Digester without baffles with 46 RPM			
DT1	951	0.746	44.81
DT2	1275	0.484	54.41
DT3	1600	0.353	62.43
DT4	1985	0.255	70.37
DT5	2234	0.205	74.84
PBTD	2283	0.196	75.66
Outlet	2268	0.201	75.36

Figure 2B shows that the overall velocity vectors for the digester design with baffles and with agitator stoppage i.e., at 0 rpm. It can be observed that the dominant radial jet with an average velocity magnitude of 0.38 m/s is only visible from the slurry inlet duct. Due to the agitator stoppage, there is no additional momentum generated inside the digester. The velocity magnitudes in the major portion of the digester are always less than 0.38 m/s. The stationary agitator acts like an additional baffle system that elicited negligible disturbances in the principal flow profile for this particular design. Figure 2C shows that the overall velocity vectors for the digester design without (w/o) baffles and agitator rotating at 46 rpm. Similar to baffled digester design, it can be observed that the radial jet from the DT impellers hits and dissipates energy near the digester wall region. However, the diverted jet will move freely in tangential direction along the digester wall because of the absence of vertical baffles. The vector plot from figure 2C depicts swirl vortices in the tangential direction. This is due to the combined effect of radial jet generated by DT impellers and centrifugal force of rotation of agitator in the absence of vertical baffles. This is also evident from the flow visualization experiments that formed a vortex flow in the free surface.

Table 1 shows the predicted pumping efficiency of the agitator rotating at 46 rpm for the digester design with and without baffles. The agitator power number, (N_p), for the digester design with baffles is greater than the design without baffles (Table 1). The vertical baffle design creates additional turbulence due to the excess energy dissipation generated by the diverted radial jets from the radial type impellers and baffle interaction. On the other hand, power number of PBTD,N_P, for the digester design without baffles is smaller than the design with baffles. The PBTD in the design without baffles creates an axial jet towards the digester wall by converting the radial jet of radial impeller (DT5) to axial jet (Figure 1C). Further, the combined axial jet flow increased the primary efficiency of PBTD to 0.957 for the design without baffle (Table 1). The efficiency of radial flow type impellers (DT) is higher for the design without baffles (Figure 3) with lesser power consumption. This is due to the tangentially directed bulk convective flow pattern along the direction of agitator rotation. The lesser cross flows in the design without baffles reduced the power consumption and improved the radial pumping efficiency of the agitator.

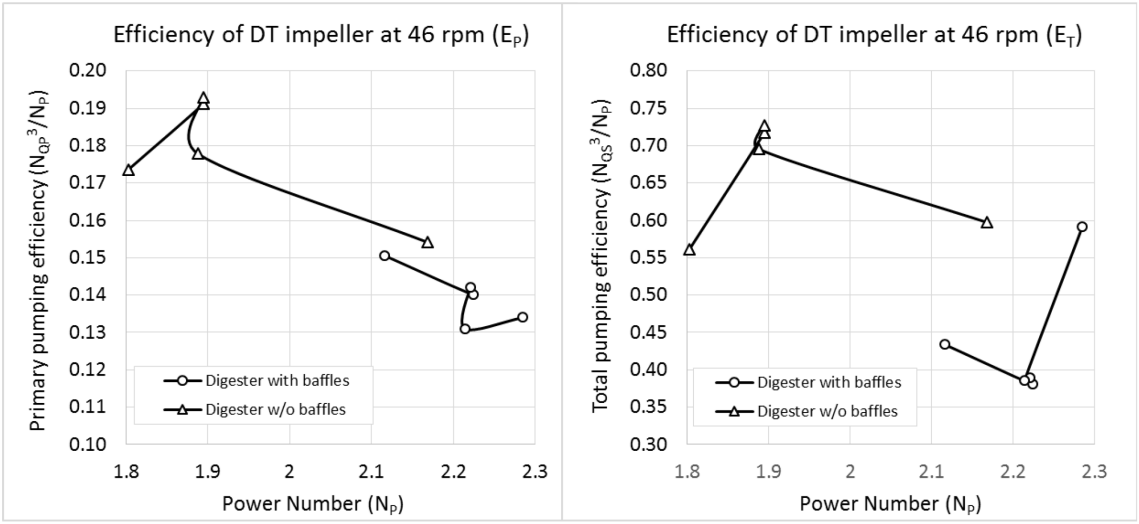

Figure 3. Pumping efficiency of DT impellers by CFD.

Figure 4 depicts the residence time distribution behaviour of the digesters using CFD studies. Additionally, Table 2 shows the quantitative comparison of retention time and dispersion number. The above flow analysis revealed that the better agitator pumping efficiency and reduced power consumption are obtained from the design without baffles. However, it is important to investigate for an optimal design that gives retention time with lesser coefficient of variance and dispersion levels along with reduced channelling and tail. More channelling will bypass the fresh bauxite slurry to the outlet causing the loss of bauxite to the red mud. Also, longer tail indicates reduction of effective volume for the given design. Both channelling and tail are the features of industry scale reactor design and it is important to minimize the loss of bauxite to red mud. The predicted retention time and dispersion number of the digester with baffle and with 46 rpm is found to be 2076 s and 0.189 respectively. However, the same design with agitator stoppage predicted with lesser retention time (2002 s) and higher dispersion number (0.215). This clearly indicates the effect of increased channelling for the digester with baffle with 0 RPM. This is also evident from figure 4. Also, it is important to note that the dispersion number for the digester with baffle with 0 RPM is highest of all the three designs considered in the present study (Table 2). This is due to the bulk axial convective flow that produced a longer axial mixing loop (Figure 2B).

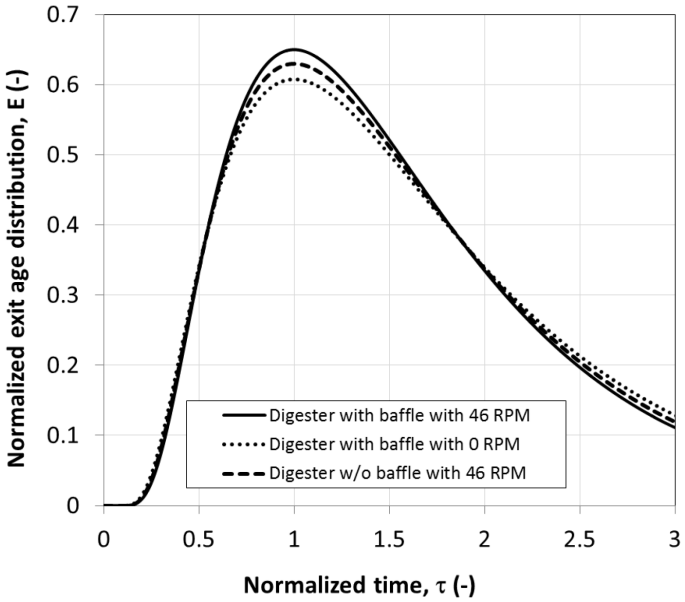

Figure 4. Residence time distribution (RTD) curves by CFD.

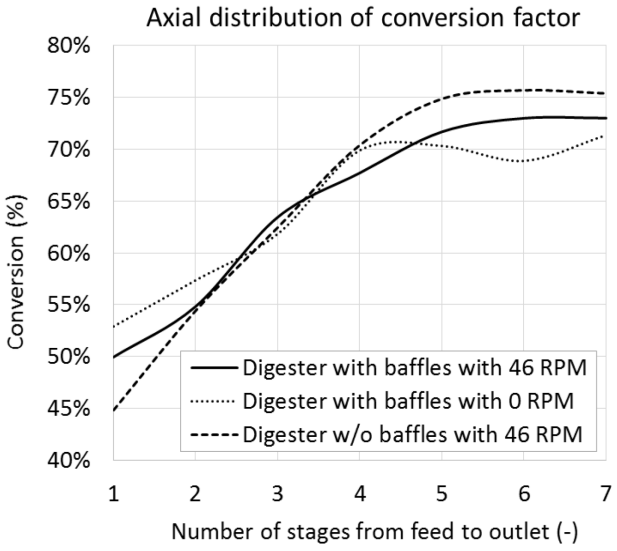

Figure 5. Axial distribution of conversion factor.

The extent of reaction is calculated using equation 11. Figure 5 shows the plot of conversion or extent of reaction. The mean retention time and dispersion number that are design dependent and are obtained from CFD

analysis. The x-axis values 1-5 in the Figure 5 shows the number of stages or volumes occupied around each impellers and the value 7 indicates the outlet. The digester design without (w/o) baffles and agitator rotating at 46 rpm shows a uniform increase in the conversion from the inlet to outlet along with maximum level of conversion. Also table 3 shows the quantitative comparison of conversion percentage for all the three digester designs.

Table 4. Validation of CFD by flow visualization experiments for the design w/o baffles.

Technique	Agitator power number, $\langle N_P \rangle$	Primary flow number of DT2, N_{QP}
Model predictions	10.81	0.713
Flow experiments	9.52	0.701

Table 4 shows the comparison of model predicted power and flow variables against the measured flow visualization experiments. The good comparison of predicted and measured values demonstrate the strength of CFD model.

6. Conclusions

The high temperature digestion is a vital unit process, extracting aluminium hydroxide from the the bauxite mineral boehmite. The agitation is found to be extremely important for high temperature digesters for better dispersion of bauxite particles in the caustic liquor. An optimum retention time is mandatory in the top section of the reactor for better heat transfer from the steam to slurry. Further, hydrodynamics with minimum bulk axial recirculation is mandatory for alumina digester design to obtain retention time with minimum standard deviation and optimum dispersion. The digester design without baffles along with an agitator rotation reduced the standard deviation around the mean retention time and improved the overall conversion, which eventually increase the extraction efficiency for the given grade of bauxite feed.

7. Abbreviations

CFD Computational fluid dynamics
DT Radial pumping impeller (Disc turbine)
PBTD Axial pumping impeller (pitched blade turbine down flow)
RTD Residence time distribution
w/o Digester design without baffles

8. Nomenclature

B_T DT periphery plane axial location at blade width (m)
B_{TE} DT periphery plane entrained flow axial location above blade width (m)
B_B DT periphery plane axial location at blade width (m)
B_{BE} DT periphery plane entrained flow axial location below blade width (m)
D Impeller diameter (m)
ϵ Energy dissipation rate (W m^{-3})
G_k Generation of k due to mean velocity gradient (kg m^{-1} s^{-3})
G_b Generation of k due to buoyancy (kg m^{-1} s^{-3})
k Turbulent kinetic energy (m^2 s^{-2})
κ Boehmite reaction rate constant (s^{-1})
L Characteristic length (m)
θ Tangential coordinate location (-)
N Agitator rotation speed (rpm)
μ Dynamic viscosity (kg m^{-1} s^{-1})
μ_t Eddy viscosity (kg m^{-1} s^{-1})
η Eddy life (s)
$\langle P \rangle$ Agitator power consumption (W)
ρ Slurry density (kg m^{-3})
r Radial coordinate location (m)
R_I PBTD axial plane impeller radius location (m)
R_R PBTD axial plane entrained flow radius location (m)

S_ϵ Source term of energy dissipation (kg m^{-1} s^{-3})
S_k Source term of k (kg m^{-1} s^{-3})
σ Standard deviation of tracer (s)
t Time (s)
T Tank diameter (m)
t_m Mean residence time (s)
τ Agitator torque (Nm)
u Characteristic velocity (m s^{-1})
U_r Mean radial velocity (m s^{-1})
U_z Mean axial velocity (m s^{-1})
V Volume of digester (m^3)
Y_M Dilatation dissipation factor (kg m^{-1} s^{-3})
z Axial coordinate location (m)

9. Dimensionless groups

D/uL Dispersion number
E Exit age distribution function
E_P Primary pumping efficiency of an impeller
E_T Total pumping efficiency of an impeller
H/T Aspect ratio of digester
σ_t Coefficient of variance (σ/t_m)
σ_k Turbulent Prandtl number for k
N_P Impeller power number
$\langle N_P \rangle$ Agitator power number
N_{QP} Primary flow number
N_{QS} Secondary flow number
P/V Power per unit volume

10. References

1. Kumaresan, T., Nere, N. K. and Joshi, J. B., "Effect of Internals on the Flow Pattern and Mixing in Stirred Tanks", Ind. Eng. Chem. Res., 44, 2005, pp 9951-9961.
2. Kumaresan et al., "Performance improvement of alumina digestors", *Seventh International Conference on CFD in the Minerals and Process Industries,* 9-11 December, 2009, CSIRO, Melbourne, Australia.
3. Rousseaux, J.-M. et al., "CFD Simulation of Precipitation in the Sliding-Surface Mixing Device", Chem. Eng. Sci., 56, 2001, pp 1677- 1685.
4. Woloshyn, J. et al., "Digestor design using CFD", Light Metals 2006, pp 939-944.
5. Kumaresan, T. and Thakre, S., "Characterization of flow, mixing and particle suspension in alumina draft tube precipitators of taller aspect ratio", Hydrometallurgy, 150, 2014, pp 107 – 122.
6. Farrow, J. B. et al., "Recent Developments in Techniques and Methodologies for Improving Thickener Performance", Chem. Eng. J., 80, 2000, pp 149-155.
7. LevenspielL, O., Chemical Reaction Engineering, 3rd Ed., (New York, NY: Wiley, 1999).
8. Scotford, R. F. and Glastonbury, J. R., (1971),"Effect of temperature on the rates of dissolution of gibbsite and boehmite, The Canadian J. of Chem. Engineering., 49, 611 – 616.
9. Addaimensah, J., Dawe, J., Ralston, J., "Dissolution and interactions of gibbsite in alkaline media", XXI Int. Min. Proc. Congress, 23 – 27 July, 2000 Rome, Italy, C6-1 – C6-7.